APPLIED PHYSICS LETTERS

Articles published week of 9 March 2009
Vol. 94, No. 10
CODEN: APPLAB ISSN: 0003-6951

► **Cover image** *from Guozhu Sun, Xueda Wen, Yiwen Wang, Shanhua Cong, Jian Chen, Lin Kang, Weiwei Xu, Yang Yu, Siyuan Han, and Peiheng Wu, Appl. Phys. Lett.* ***94****, 102502 (2009).*

LASERS, OPTICS, AND OPTOELECTRONICS

PLASMAS AND ELECTRICAL DISCHARGES

(Continued)

STRUCTURAL, MECHANICAL, THERMODYNAMIC, AND OPTICAL PROPERTIES OF CONDENSED MATTER

(Continued)

ELECTRONIC TRANSPORT AND SEMICONDUCTORS

MAGNETISM AND SUPERCONDUCTIVITY

(Continued)

DIELECTRICS AND FERROELECTRICITY

(Continued)

(Continued)

(Continued)

Practical enhancement of photoluminescence by metal nanoparticles

G. Sun,[1,a] J. B. Khurgin,[2] and R. A. Soref[3]
[1]*Department of Physics, University of Massachusetts Boston, Boston, Massachusetts 02125, USA*
[2]*Department of Electrical and Computer Engineering, Johns Hopkins University, Baltimore, Maryland 21218, USA*
[3]*Sensors Directorate, Air Force Research Laboratory, Hanscom AFB, Massachusetts 01731, USA*

(Received 22 January 2009; accepted 12 February 2009; published online 9 March 2009)

We develop a simple yet rigorous theory of the photoluminescence (PL) enhancement in the vicinity of metal nanoparticles. The enhancement takes place during both optical excitation and emission. The strong dependence on the nanoparticle size enables optimization for maximum PL efficiency. Using the example of InGaN quantum dots (QDs) positioned near Ag nanospheres embedded in GaN, we show that strong enhancement can be obtained only for those QDs, atoms, or molecules that are originally inefficient in absorbing as well as in emitting optical energy. We then discuss practical implications for sensor technology. © *2009 American Institute of Physics*.
[DOI: 10.1063/1.3097025]

The enhancement of luminescence from various optically active objects of nanoscale dimensions such as atoms, molecules, and quantum dots (QDs) (here we shall use the generic term "molecule" to donate them all) when placed in close proximity to metal nanoparticles[1–10] is a phenomenon that has been conceptually well understood as a product of strong localized electric field induced by the surface plasmons (SPs).[11] This enhancement with important applications in sensing has been attributed primarily to the increase in radiative decay rate caused by the Purcell[12] effect associated with the tightly confined high-density SP modes. That treatment is adequate in estimating the enhancement factor for electroluminescence where the excitation energy in the form of an electric dipole gets coupled directly into the SP modes. But for photoluminescence (PL), the situation is more complicated. There are two enhancement mechanisms at work. One takes place during the optical excitation stage and the other during the stage of light emission. In the absence of metal nanoparticles, the optical excitation typically in the form of a focused laser beam is being absorbed by the molecules. With a metal nanoparticle placed in the vicinity of the molecules, the beam can now get coupled first into the tightly confined SP mode enhancing the optical energy density near the molecule field, which enhances the absorption rate. The same SP modes (albeit at different frequencies) can also enhance the energy-emission efficiency of the excited molecules through the Purcell[12] effect. A proper estimate of PL enhancement by metal nanoparticles therefore has to include both energy absorption and emission processes that are enhanced simultaneously by the associated SP modes. To make the matter even more complicated, all of these processes depend on the wavelength relationships between the optical excitation, the molecule emission, and the SP mode. A clear understanding of the enhancement mechanism is obviously important for improving the performance of sensors relying upon PL. Based on the "effective mode volume" approach,[13] we have previously developed analytical models that rigorously treated the enhancement effects of light emission by molecules in the presence of a metal sheet[14] and metal nanoparticles,[15] as well as light absorption by molecules in the proximity of metal nanoparticles.[16] Combining the models for light absorption[16] and emission by metal nanoparticles,[15] we are now in position to calculate how much total enhancement one can realistically obtain in measured PL for a given metal embedded in a given dielectric medium. We can also provide an analytical approach for optimizing the metal nanostructure in order to achieve maximum enhancement. The salient feature of our approach is that it shows the attainable PL enhancement that can be optimized for each particular molecule—characterized by the absorption cross section at the excitation frequency $\sigma_a(\omega_{ex})$, the radiative efficiency $\eta_{rad}(\omega_{PL})$, and their product—the PL cross section $\sigma_{PL}(\omega_{ex},\omega_{PL})=\sigma_a(\omega_{ex})\eta_{rad}(\omega_{PL})$.

The enhancement of a PL process is illustrated in Fig. 1. Optical excitation at the frequency of ω_{ex} in the form of a laser beam is focused into the region where a metal nanosphere with a radius r and a molecule separated by a distance d are located. The excitation beam couples into the highly confined SP mode around the metal sphere with an incoupling coefficient κ_{in}. Energy inside the SP mode is then absorbed by the active molecule with an absorption cross section σ_a. This process competes with radiative (γ_{rad}) and nonradiative decays (γ_{nrad}) of the SP mode. The excited mol-

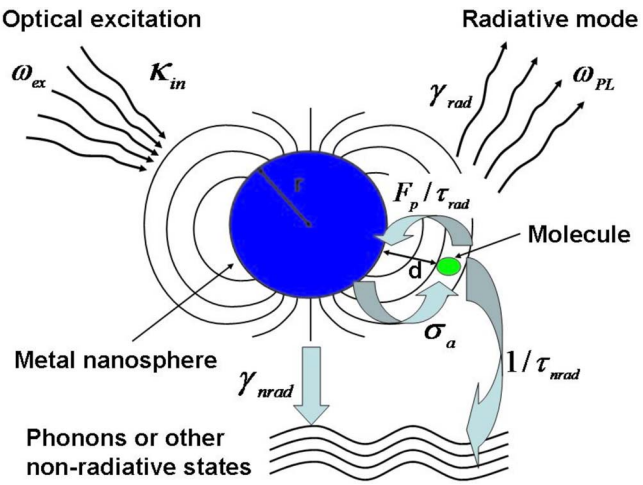

FIG. 1. (Color online) Illustration of the enhancement of a PL process by the incoupling of the optical excitation into the SP mode surrounding a metal sphere and by the outcoupling of the SP mode into the radiative mode.

[a]Electronic mail: greg.sun@umb.edu.

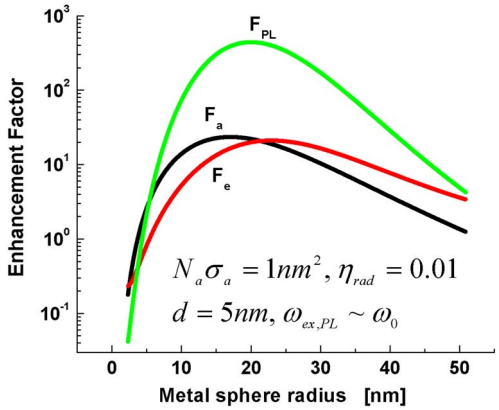

FIG. 2. (Color online) Absorption F_a, emission F_e, and total enhancement factors F_{PL} vs metal sphere radius for Ag/GaN.

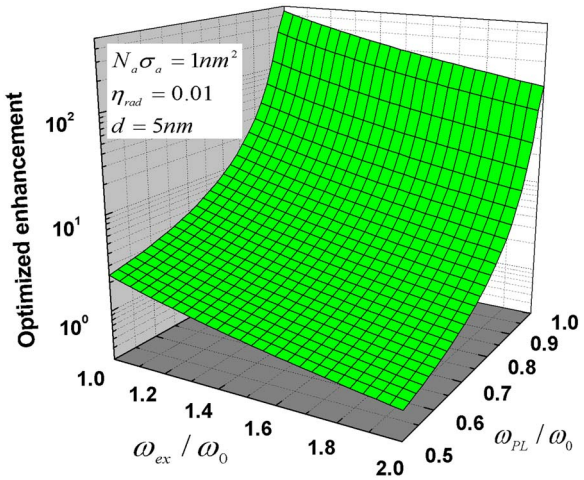

FIG. 3. (Color online) Optimized PL enhancement factor vs frequency detuning ratio of the optical excitation $\omega_{\mathrm{ex}}/\omega_0$ and PL emission $\omega_{\mathrm{PL}}/\omega_0$.

ecule with the original radiative decay rate $1/\tau_{\mathrm{rad}}$ subsequently relaxes by emitting energy at the frequency ω_{PL} into the SP mode at the rate of F_P/τ_{rad}, which is enhanced by the Purcell[12] factor F_P. Simultaneously, the molecule also relaxes into nonradiative modes at its original nonradiative rate of $1/\tau_{\mathrm{nrad}}$. The observed PL power depends on the outcoupling efficiency of the SP mode $\eta_{\mathrm{pr}}=\gamma_{\mathrm{rad}}/(\gamma_{\mathrm{rad}}+\gamma_{\mathrm{nrad}})$. It is clear that strong PL enhancement occurs when the frequencies of both optical excitation and emission are close to the SP resonance. It is thus optimal to have the frequency relationship $\omega_{\mathrm{ex}}\geq\omega_0\geq\omega_{\mathrm{PL}}$ for PL measurement.

Following our previous work,[16] we first treat the enhancement of absorption by a metal nanosphere. In the absence of the metal nanosphere, the optical excitation will simply be focused onto a diffraction limited spot at the apex of the cone characterized by a far field half angle θ with a spot radius at the waist $w_0=\lambda_{\mathrm{ex}}/\pi\theta$, where λ_{ex} is the excitation wavelength in the dielectric medium. The electric field in the focal spot E_{foc} is related to the power $|s_+|^2$ carried by the incident wave as $|s_+|^2=\pi n w_0^2 E_{\mathrm{foc}}^2/4Z_0$, where Z_0 is the impedance of free space and n is the index of refraction. In the presence of a metal sphere with radius r, the incident light gets coupled into the SP mode with an incoupling coefficient $\kappa_{\mathrm{in}}\approx\theta\sqrt{3\gamma_{\mathrm{rad}}/8}$.[17] The SP mode has a maximum field E_{max} at the surface of the sphere that is related to its energy $|a|^2=\frac{1}{2}\varepsilon_0\varepsilon_D E_{\mathrm{max}}^2 V_{\mathrm{eff}}$, where ε_0 is the permittivity of free space, ε_D is the dielectric constant of the medium, and $V_{\mathrm{eff}}=(4\pi r^3/3)[1+(2\varepsilon_D)^{-1}]$ is the effective mode volume at the resonant frequency ω_0 (wavelength λ_D in the dielectric).[15] The field enhancement is then found from the steady-state solution of the rate equation for the amplitude a of the SP mode that describes the incoupling of the incident wave at the excitation frequency ω_{ex} and the various decay mechanisms,[13]

$$\frac{da}{dt}=j(\omega_{\mathrm{ex}}-\omega_0)a-\frac{1}{2}(\gamma_{\mathrm{rad}}+\gamma_{\mathrm{nrad}}+\gamma_{\mathrm{abs}})a+\kappa_{\mathrm{in}}s_+, \qquad (1)$$

where γ_{nrad} is the rate due to the Ohmic loss in the Drude model approximation, $\gamma_{\mathrm{rad}}=[\omega_0/(1+2\varepsilon_D)](2\pi r/\lambda_D)^3$ is the radiative decay rate in the dipole approximation,[15] and $\gamma_{\mathrm{abs}}=(cN_a\sigma_a/nV_{\mathrm{eff}})[r/(r+d)]^6$ is the decay rate due to energy absorption by N_a molecules placed near the sphere. Introducing the Q-factors for the nonradiative decay as $Q_n=\omega_0/[(1+2\varepsilon_D)\gamma_{\mathrm{nrad}}]$, for absorption as $Q_a=\omega_0/[(1+2\varepsilon_D)\gamma_{\mathrm{abs}}]$, and the normalized excitation detuning as $\delta_{\mathrm{ex}}=2(1+2\varepsilon_D)|\omega_{\mathrm{ex}}-\omega_0|/\omega_0$, and taking into account that molecules are situated at a distance d away from the metal sphere, we arrive at the energy density (and thus absorption) enhancement factor

$$F_a=\frac{9\varepsilon_D}{2}\left(\frac{\omega_0}{\omega_{\mathrm{ex}}}\right)^2\frac{1}{\delta_{\mathrm{ex}}^2+(\chi^3+Q_n^{-1}+Q_a^{-1})^2}\left(\frac{\chi}{\chi+\chi_d}\right)^6, \qquad (2)$$

where we have used the normalized radius $\chi=2\pi r/\lambda_D$ and distance $\chi_d=2\pi d/\lambda_D$.

Let us now turn our attention to the enhancement of the emission process. The energy in a molecule with an original radiative efficiency $\eta_{\mathrm{rad}}=\tau_{\mathrm{rad}}^{-1}/(\tau_{\mathrm{rad}}^{-1}+\tau_{\mathrm{nrad}}^{-1})$ can be coupled into the SP mode at the PL frequency ω_{PL} into the SP mode according to the rate $F_P(\omega_{\mathrm{PL}})/\tau_{\mathrm{rad}}$ where the Purcell factor $F_P(\omega_{\mathrm{PL}})$ as the ratio of the SP effective density of SP modes $\rho_{\mathrm{SP}}=[L(\omega_{\mathrm{PL}})/V_{\mathrm{eff}}][\chi/(\chi+\chi_d)]^6$ to that of the radiation continuum $\rho_{\mathrm{rad}}=8\pi/(3\lambda_{\mathrm{PL}}^3\omega_{\mathrm{PL}})$ with the Lorentzian linewidth factor $L(\omega)=[(\gamma_{\mathrm{rad}}+\gamma_{\mathrm{nrad}})/2\pi]/[(\omega-\omega_0)^2+(\gamma_{\mathrm{rad}}+\gamma_{\mathrm{nrad}})^2/4]$ is given as[15]

$$F_P(\omega_{\mathrm{PL}})=\frac{9\varepsilon_D}{\chi^3}\left(\frac{\omega_0}{\omega_{\mathrm{PL}}}\right)^2\frac{\chi^3+Q_n^{-1}}{\delta_{\mathrm{PL}}^2+(\chi^3+Q_n^{-1})^2}\left(\frac{\chi}{\chi+\chi_d}\right)^6, \qquad (3)$$

in which the normalized PL detuning $\delta_{\mathrm{PL}}=2(1+2\varepsilon_D)|\omega_{\mathrm{PL}}-\omega_0|/\omega_0$. The enhancement factor can now be evaluated as

$$F_e=\frac{1+F_P\eta_{\mathrm{pr}}}{1+F_P\eta_{\mathrm{rad}}}, \qquad (4)$$

where the radiative outcoupling efficiency of the SP mode $\eta_{\mathrm{pr}}=Q_n\chi^3/(1+Q_n\chi^3)$. Finally, combining the two sequential enhancement processes given by Eqs. (2) and (4), we arrive at the total PL enhancement factor $F_{\mathrm{PL}}=F_aF_e$ that shows a rather complicated dependence on one adjustable parameter—the size of nanoparticle χ. This dependence can be traced to the fact that nanoparticles play two mutually exclusive roles—that of antenna for efficient in- and outcoupling of energy and that of a nanocavity for energy concentration. An efficient antenna requires a large dipole, while a high concentration of energy calls for a small nanocavity. Therefore, for each combination of χ_d, N_a, σ_a, and η_{rad}, there exists an optimum size χ that maximizes PL enhancement.

It is not difficult to see that the largest enhancement can be obtained only for a small number of molecules placed very close to the metal sphere, $\chi_d\ll\chi$, with a small absorption cross section, $Q_a\gg Q_n$, and a small original radiative

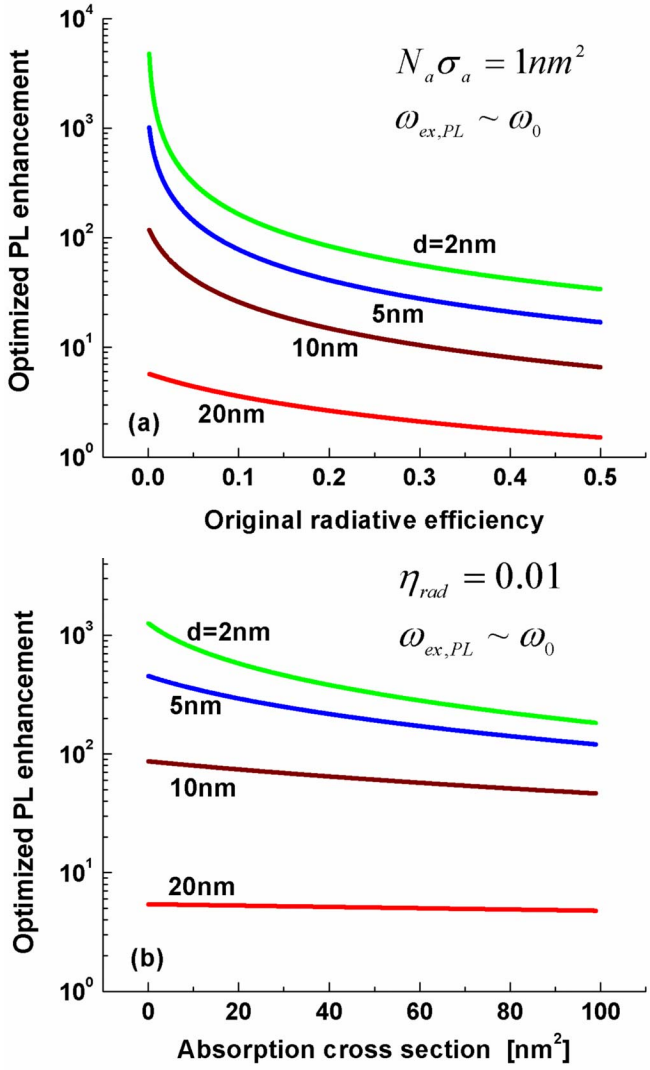

FIG. 4. (Color online) Optimized PL enhancement as a function of (a) original radiative efficiency η_{rad} at fixed $N_a\sigma_a=1$ nm^2 and (b) absorption cross section $N_a\sigma_a$ at fixed $\eta_{\text{rad}}=0.01$ for several values of the molecule-metal spacing d and near resonance optical excitation and PL emission.

efficiency, $F_P\eta_{\text{rad}} \ll 1$, when both excitation and PL frequencies are close to SP resonance, $\omega_{\text{ex,PL}} \sim \omega_0$. Under these favorable conditions, we obtain $F_{\text{PL}} \approx 81\varepsilon_D^2/[2(\chi^3+Q_n^{-1})^4]$, indicating that for a small metal sphere, $\chi^3 Q_n \ll 1$, the maximum enhancement factor $F_{\text{PL,max}} \approx 81\varepsilon_D^2 Q_n^4/2$ in line with what a simple electrostatic analysis predicts. For a Ag nanosphere embedded in GaN ($Q_n=2.77$, $\varepsilon_D=5.81$, and $\hbar\omega_0=2.344$ eV), $F_{\text{PL,max}} \approx 8.0\times 10^4$. This is a huge enhancement, but in reality, the PL enhancement is not nearly as significant when the finite absorption cross section and original radiative efficiency of the molecules that are spaced a finite distance away from the metal sphere are taken into account.

Consider the example of InGaN QDs situated at $d=5$ nm away from a Ag sphere in GaN with $N_a\sigma_a=1$ nm^2 and $\eta_{\text{rad}}=0.01$. The resulting PL enhancement factor F_{PL}, along with its enhancement contributions from absorption F_a and emission F_e, is shown in Fig. 2, where the optical excitation and emission frequencies are very close to the resonance of SP mode, $\omega_{\text{ex,PL}} \sim \omega_0$. There exists an optimized size of the metal sphere for which maximum enhancement is achieved. Also, as one can see, the two contributions are roughly of the same order. Figure 3 shows the optimized PL enhancement factor as a function of the detuning of optical excitation $\omega_{\text{ex}}/\omega_0$ and that of PL emission $\omega_{\text{PL}}/\omega_0$ for the same example—which clearly indicates that it is more critical to have the PL emission frequency near resonance with the SP mode. This is because, as shown in Fig. 4, the dependence of PL enhancement on the original radiative efficiency η_{rad} [Fig. 4(a)] is more sensitive than that on the total absorption cross section $N_a\sigma_a$ [Fig. 4(b)]. It is clear that PL enhancement is strong only if the active molecules are both weak absorbers and inefficient emitters being positioned in close proximity to the metal nanoparticles. Note that the condition $\sigma_a\eta_{\text{rad}} \to 0$ under which the maximum enhancement is achieved is always satisfied for Raman scattering, which can be seen as nothing but PL with a negligibly small cross section; hence $F_{\text{Raman}} \approx F_{\text{PL,max}}$. Indeed the experimentally verified enhancement of Raman scattering is always significantly larger than that for PL.

In summary, we have analytically treated the PL enhancement as a product of two equally important factors—one on the absorption stage and another on the emission stage—and for a given metal-dielectric combination there exists an optimal nanoparticle size that maximizes the combined enhancement. The key conclusion is that metal nanoparticles provide large PL enhancement only for small quantities of the atoms, molecules, or QDs with originally low PL cross section, hence metal nanoparticles can be indispensable in improving sensors but are of limited use in other applications, where PL is already reasonably (a few percent) efficient.

[1] P. J. Schuck, D. P. Fromm, A. Sundaramurthy, G. S. Kino, and W. E. Moerner, Phys. Rev. Lett. **94**, 017402 (2005).
[2] J.-Y. Wang, Y.-W. Kiang, and C. C. Yang, Appl. Phys. Lett. **91**, 233104 (2007).
[3] S. Kühn, U. Håkanson, L. Rogobete, and V. Sandoghdar, Phys. Rev. Lett. **97**, 017402 (2006).
[4] R. Carminati, J.-J. Greffet, C. Henkel, and J. M. Vigoureux, Opt. Commun. **261**, 368 (2006).
[5] L. Rogobete, H. Schniepp, V. Sandoghdar, and C. Henkel, Opt. Lett. **28**, 1736 (2003).
[6] C. Girard, O. J. F. Martin, and A. Dereux, Phys. Rev. Lett. **75**, 3098 (1995).
[7] L. Novotny, Appl. Phys. Lett. **69**, 3806 (1996).
[8] M. Thomas, J.-J. Greffet, R. Carminati, and J. R. Arias-Gonzalez, Appl. Phys. Lett. **85**, 3863 (2004).
[9] G. Baffou, C. Girard, E. Dujardin, G. C. des Francs, and O. J. F. Martin, Phys. Rev. B **77**, 121101(R) (2008); G. Colas des Francs, C. Girard, T. Laroche, G. Leveque, and O. J. F. Martin, J. Chem. Phys. **127**, 034701 (2007).
[10] R. M. Bakker, V. P. Drachev, Z. Liu, H.-K. Yuan, R. H. Pedersen, A. Boltasseva, J. Chen, J. Irudayaraj, A. V. Kildishev, and V. M. Shalaev, New J. Phys. **10**, 125022 (2008).
[11] D. Maystre, in *Electromagnetic Surface Modes*, edited by A. D. Boardman (Wiley, New York, 1982), Chap. 17.
[12] M. Purcell, H. C. Torrey, and R. V. Pound, Phys. Rev. **69**, 37 (1946).
[13] S. Maier, Opt. Express **14**, 1957 (2006).
[14] J. B. Khurgin, G. Sun, and R. A. Soref, J. Opt. Soc. Am. B **24**, 1968 (2007); G. Sun, J. B. Khurgin, and R. A. Soref, Appl. Phys. Lett. **90**, 111107 (2007).
[15] J. B. Khurgin, G. Sun, and R. A. Soref, Appl. Phys. Lett. **93**, 021120 (2008); G. Sun, J. B. Khurgin, and R. A. Soref, J. Opt. Soc. Am. B **25**, 1748 (2008).
[16] J. B. Khurgin, G. Sun, and R. A. Soref, Appl. Phys. Lett. **94**, 071103 (2009).
[17] H. A. Haus, *Waves and Fields in Optoelectronics*, 1st ed. (Prentice-Hall, Englewood Cliffs, NJ, 1984).

Photoluminescence enhancement by gold nanoparticles in Eu^{3+} doped $GeO_2-Bi_2O_3$ glasses

Luciana R. P. Kassab,[1] Diego S. da Silva,[2] Ricardo de Almeida,[2] and Cid B. de Araújo[3,a)]
[1]*Laboratório de Vidros e Datação, Faculdade de Tecnologia de São Paulo (FATEC-SP, CEETEPS), São Paulo, São Paulo 01124-060, Brazil*
[2]*Departamento de Engenharia de Sistemas Eletrônicos, Escola Politécnica da USP, São Paulo, São Paulo 05508-900, Brazil*
[3]*Departamento de Física, Universidade Federal de Pernambuco, Recife, Pernambuco 50670-901, Brazil*

(Received 6 January 2009; accepted 18 February 2009; published online 11 March 2009)

We report large photoluminescence (PL) enhancement in Eu^{3+}-doped $GeO_2-Bi_2O_3$ glasses containing gold nanoparticles (NPs). Growth of ≈1000% in the PL intensity corresponding to the Eu^{3+} transition $^5D_0 \rightarrow {}^7F_2$, at 614 nm, was observed in comparison with a reference sample that does not contain gold NPs. Other PL bands from 580 to 700 nm are also enhanced. The enhancement of the PL intensity is attributed to the increased local field in the Eu^{3+} locations due to the presence of the NPs and the energy transfer from the excited NPs to the Eu^{3+} ions. © *2009 American Institute of Physics*. [DOI: 10.1063/1.3097241]

To enhance the photoluminescence (PL) properties of glasses doped with rare-earth ions (REI), samples containing metal nanoparticles (NPs) have been investigated by various authors.[1–5] The increase of the local field due to the NPs has been accounted as a possible cause for the PL enhancement. Because of the mismatch between the dielectric function of the metallic NPs and the host glass, there is a confinement of the electromagnetic field near the NPs' surface originating enhanced near-field intensities. Then the REI located nearby the metallic NPs contribute for the enhanced PL. Another possible way for PL enhancement involves the absorption of light by the NPs followed by energy transfer to the REI. Since the light absorption cross section of the NPs is larger than for the REI, this PL excitation route may be more efficient in some cases.

The PL enhancement factor (the ratio between the luminescence intensity from samples with and without metallic NPs) η depends on the volume fraction of the sample occupied by the NPs, the so-called filling fraction, and light wavelength. When the incident light or the PL has wavelength close to the NPs surface plasmons (SPs) resonance wavelength λ_{SP}, the factor η can be considerably large. The value of λ_{SP} depends on the host and the metal dielectric functions, as well as on the size and shape of the NPs.[1,2]

Since heavy-metal oxide glasses are suitable materials for photonic devices, we have studied their PL properties using REI doped samples containing silver and gold NPs.[6–10] Heavy-metal oxide glasses present high refractive index and broad transparency window from the visible to the middle infrared. When doped with REI heavy-metal oxide glasses become highly luminescent due to the low cutoff phonon energy of the host matrix that significantly decreases nonradiative transition rates of the REI electronic levels in comparison with other glasses.

Nucleation of silver NPs was reported for Pr^{3+} doped GeO_2-PbO glasses, and PL enhancement was observed for samples with different concentrations of Pr^{3+} and silver NPs.[6,7] Intensified infrared-to-visible frequency upconversion in Er^{3+} doped GeO_2-PbO glasses containing silver NPs was observed corresponding to $\eta \approx 100\%$ for PL in the green region.[8] The influence of silver NPs was exploited to obtain enhancement of the whole frequency upconversion spectra from 500 to 700 nm in $Yb^{3+}-Er^{3+}$ doped GeO_2-PbO glasses.[9] The increase of Eu^{3+} luminescence due to the presence of gold NPs in tellurite glasses was reported in Ref. 10. The Eu^{3+} hypersensitive transition $^5D_0 \rightarrow {}^7F_2$ at 614 nm was enhanced by ~100%.

Due to the increasing use of Eu^{3+} in photonic applications, other glass matrices have to be investigated for identification of more appropriate hosts. Therefore, in this letter, we report on the characteristics of Eu^{3+}-doped $GeO_2-Bi_2O_3$ glass containing gold NPs. This glass has been studied by other authors because of its large potential for many applications (see, for instance, Refs. 11–14). We discovered that $GeO_2-Bi_2O_3$ glass allowed more efficient nucleation of gold NPs than the previously reported materials. Consequently, an enhancement factor $\eta \approx 1000\%$ for the PL at 614 nm was obtained for samples heat treated at 420 °C for 3 h. The whole PL spectrum from 580 to 700 nm is intensified.

The samples were prepared by the melt-quenching method using the starting composition 58.4 GeO_2–41.6 Bi_2O_3 in wt %. The doping species were Eu_2O_3 (0.5 wt %) and Au_2O_3 (3.0 wt %). The reagents were melted in an alumina crucible for 1 h at 1100 °C, quenched in air in a preheated brass mold, and annealed. Heat treatment of the samples is made to minimize internal stress and to thermally reduce the Au^+ and Au^{3+} ions for nucleation of gold NPs. The samples studied were annealed at 420 °C for 3, 24, 48, and 72 h.

A 200 kV transmission electron microscope (TEM) was used to investigate the nucleation of NPs. A representative TEM image is presented in Fig. 1 showing that gold NPs and some NPs' aggregates are nucleated inside the glass.

Figure 2 shows the absorption spectra of the samples containing Eu^{3+} and gold NPs. The spectrum of a sample without gold NPs and doped with 0.5 wt % of Eu_2O_3 is shown for reference. Features associated to the Eu^{3+} $4f$-$4f$

a)Author to whom correspondence should be addressed. Electronic mail: cid@df.ufpe.br.

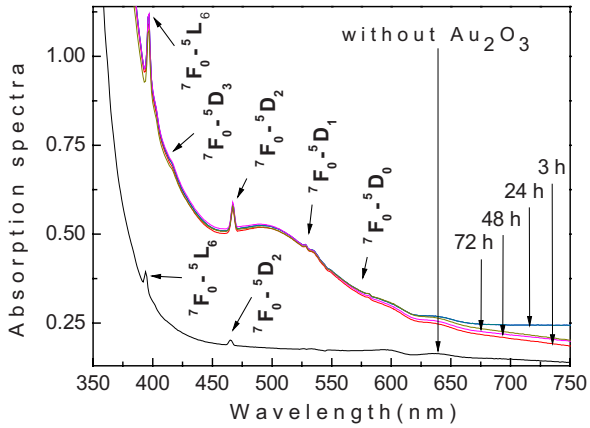

FIG. 1. (Color online) Absorption spectra of the Eu^{3+} doped GeO_2–Bi_2O_3 samples heat-treated for different times.

transitions originated from the ground state ($^7F_0$) are observed. The broad absorption band centered at ≈500 nm is attributed to the SP resonance. Its amplitude does not change much with the heat-treatment time, and this indicates that all gold ions are chemically reduced for 3 h of heat treatment. Note that some Eu^{3+} transitions overlap with the SP band.

PL was excited using a 15 W xenon lamp followed by a 0.25 m monochromator equipped with a holographic grating. The spectra obtained for excitation at 405 nm, in resonance with the Eu^{3+} transition $^7F_0$-$^5D_3$, is shown in Fig. 3. The emission bands centered in ≈585, ≈595, ≈614, ≈655, and ≈700 nm, correspond to Eu^{3+} transitions $^5D_0$-^7F_J (J=0, 1, 2, 3, and 4). A simplified energy level scheme for the Eu^{3+} ions and the optical transitions observed in Fig. 3 are indicated in Fig. 4.

The results of Fig. 3 indicate that the PL bands are affected by the presence of gold NPs. For instance, the signal centered at 614 nm, for the samples heat-treated for 3 h, is approximately ≈10 times larger than the signal observed for the sample that does not contain gold NPs. Since the incident light can be absorbed by the NPs, we attribute the PL increase not only to the enhanced local field but also to energy transfer from the NPs to the Eu^{3+} ions. PL enhancement is partially due to the increased Eu^{3+} absorption due to the gold

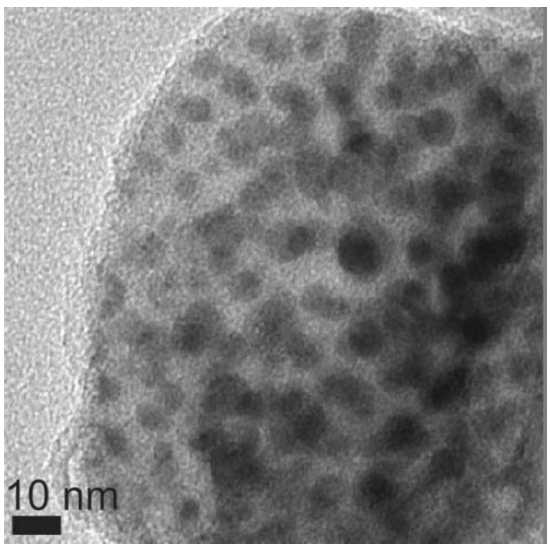

FIG. 2. TEM image of the sample heat treated for 24 h.

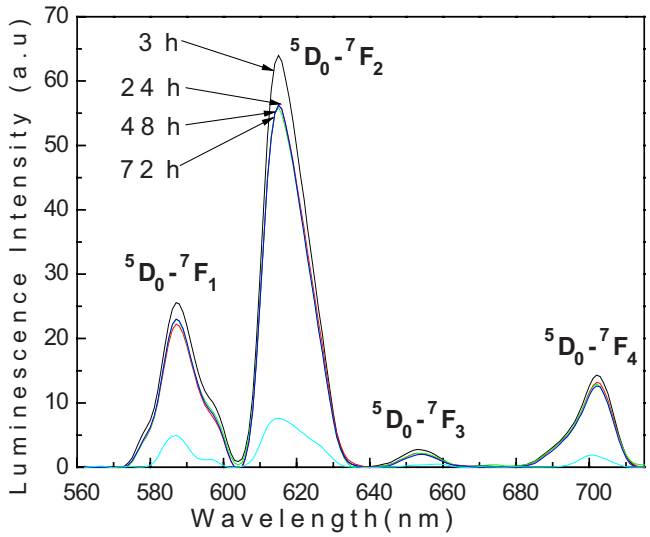

FIG. 3. (Color online) PL spectra of the samples heat-treated for different times (excitation at 405 nm). The spectrum for the sample doped with 0.5 wt % of Eu_2O_3 and no metal NPs is also shown to illustrate the luminescence enhancement.

NPs. Note that the amplitude of the $^7F_0$-$^5D_2$ transition in Fig. 1 is larger in the heat-treated samples. On the other hand, the dependence with the PL wavelength is clear because the bands associated to the electric-dipole transitions $^5D_0$-$^7F_{2,4}$ increased by ≈1000% while the magnetic-dipole transitions $^5D_0$-$^7F_{1,3}$ increased by ≈500%. The other transitions are enhanced by different factors. The small PL quenching observed for heat treatments longer than 3 h is probably because, with the increasing of the heat-treatment time, more Eu^{3+} ions become so near from the NPs that energy transfer occurs from the directly excited ions to the NPs. This is expected when the distance between the REI and the NPs is smaller than 5 nm because at short distances the dipole-dipole interaction between REI and NP becomes large.[1] Therefore we should consider that most of the excited NPs transfer the absorbed energy to the glass matrix. Measurements with Eu^{3+}-doped samples without gold NPs do not

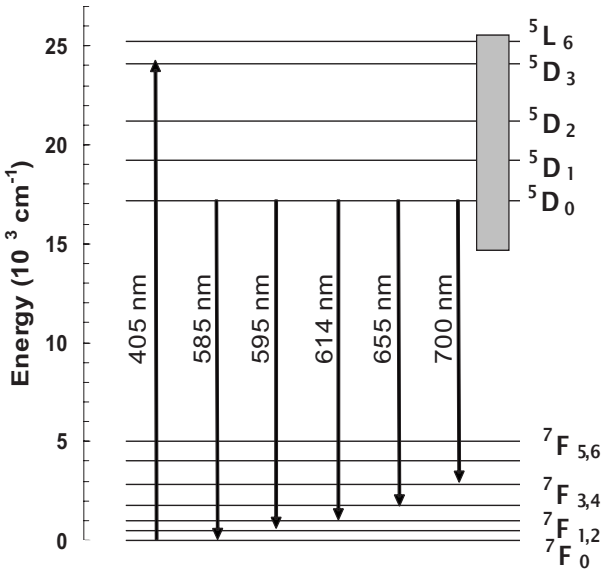

FIG. 4. Simplified energy levels scheme of Eu^{3+} ions with indication of the radiative transitions observed. The shaded area indicates the SPs band location.

show dependence of PL signals with the heat treatment demonstrating the essential role due to the NPs.

In summary, the present results show that the nucleation of gold NPs in Eu^{3+} doped $GeO_2-Bi_2O_3$ glass is more efficient than in tellurite glasses. Because larger gold NPs filling fractions are obtained the PL enhancement in the orange-red spectral region is the largest observed for the different glasses previously studied.

We acknowledge the support from Conselho Nacional de Desenvolvimento Científico e Tecnológico (CNPq) and Fundação de Amparo a Ciência e Tecnologia do Estado de Pernambuco (FACEPE). The Centro de Ciência e Tecnologia de Materiais do IPEN-SP is also acknowledged for the TEM images. This work was performed under the Nanophotonics Network Program.

[1]P. N. Prasad, *Nanophotonics* (Wiley, New York, 2004).
[2]M. Yamane and Y. Asahara, *Glasses for Photonics* (Cambridge University Press, Cambridge, UK, 2000), and references therein.
[3]O. L. Malta, P. A. S. Cruz, G. F. de Sá, and F. Auzel, J. Lumin. **33**, 261 (1985).
[4]C. Strohhöfer and A. Polman, Appl. Phys. Lett. **81**, 1414 (2002).
[5]G. Fu, W. Cai, C. Kan, C. Li, and L. Zhang, Appl. Phys. Lett. **83**, 36 (2003).
[6]L. P. Naranjo, C. B. de Araújo, O. Malta, P. A. S. Cruz, and L. R. P. Kassab, Appl. Phys. Lett. **87**, 241914 (2005).
[7]L. R. P. Kassab, C. B. de Araújo, R. A. Kobayashi, R. de Almeida Pinto, and D. M. da Silva, J. Appl. Phys. **102**, 103515 (2007).
[8]D. M. da Silva, L. R. P. Kassab, S. R. Lüthi, C. B. de Araújo, A. S. L. Gomes, and M. J. V. Bell, Appl. Phys. Lett. **90**, 081913 (2007).
[9]L. R. P. Kassab, F. A. Bonfim, J. R. Martinelli, N. U. Wetter, J. J. Neto, and C. B. de Araújo, Appl. Phys. B: Lasers Opt. **94**, 239 (2009).
[10]R. de Almeida, D. M. da Silva, L. R. P. Kassab, and C. B. de Araújo, Opt. Commun. **281**, 108 (2008).
[11]R. Balda, J. Fernández, M. Sanz, A. de Pablos, J. M. Fdez-Navarro, and J. Mugnier, Phys. Rev. B **61**, 3384 (2000).
[12]L. Baia, J. Mol. Struct. **599**, 9 (2001).
[13]A. B. Meshalkin and A. B. Kaplun, J. Cryst. Growth **275**, e905 (2005).
[14]S. Dong-Mei, Q. Y. Zhang, G. F. Yang, Y. H. Liu, and Z. H. Jiang, Chin. Phys. Lett. **23**, 478 (2006).